

# CRYOGENIC IMAGING X-RAY SPECTROMETER

R.J. Wiegerink, J.J. van Baar, J.H. de Boer,  
MESA+ Institute, University of Twente, P.O. Box 217, 7500 AE Enschede, The Netherlands

M.L. Ridder, M.P. Bruijn, A. Germeau, H.F.C. Hoevers  
SRON National Institute for Space Research, Sorbonnelaan 2, 3584 CA Utrecht, The Netherlands

## ABSTRACT

A micro-calorimeter array consisting of superconducting transition-edge sensors is under development for the X-ray imaging spectrometer on board of ESA's XEUS (X-ray Evolving Universe Spectroscopy) mission. An array of 32 x 32 pixels with a pixel size of 250 micron square is envisaged. So far, 5 x 5 pixels arrays were successfully fabricated along two fabrication routes: a bulk micromachining and a surface micromachining route. Both routes result in working arrays with energy resolutions down to 5 eV FWHM for the best pixels.

## 1. INTRODUCTION

One of the future missions in space-based astronomy is ESA's XEUS (X-ray Evolving Universe Spectroscopy) mission with a high-resolution imaging X-ray detector being one of the main instruments. Requirements for this detector are an energy resolution of 2 eV for 1 keV photons and 5 eV for 7 keV photons, a time constant smaller than 100  $\mu$ s, and high absorption efficiency (>90% up to 7 keV). Since the initial conception of X-ray micro-calorimeters [1], several new types have been proposed with the Transition Edge Sensor (TES) [2] being one of the most promising. TESs employ superconducting-to-normal phase transition thermometers, with a critical temperature of typically 100 mK, that are operated in extreme electro-thermal feedback (ETF) through the use of voltage bias. A major advantage is that the fabrication is compatible with micromachining techniques, thereby potentially enabling the production of very large pixel arrays. ETF results in stable responsivity, fast (50-100  $\mu$ s) response time, and 2 - 4 eV energy resolution in the energy band of 1 to 10 keV. Optimum response can be tuned to an energy region of interest (from sub-mm, through visible to X-ray and gamma) by choosing an appropriate radiation absorber and thermal coupling between detector and heat bath.

## 2. DESIGN

### TES $\mu$ -Calorimeter Basics

The basic physics and theoretical performance of a voltage-biased detector with a superconducting-to-normal phase transition thermometer are well established [2, 3]. In this section we only provide the reader with the basic operating principle. Fig. 1 shows a simplified schematic of a microcalorimeter with TES readout. The structure basically

consists of a Cu/Bi radiation absorber and a Ti/Au TES thermometer with combined heat capacity  $C$ , which are coupled to a cold bath ( $\sim 20$  mK) by a thermal link, usually a  $\text{Si}_3\text{N}_4$  structure, whose thermal conductance  $G$  can be engineered to the application. The Ti/Au bi-layer is a superconductor and below the critical temperature, in this case  $\sim 100$  mK, the resistance drops from typically  $0.1 \Omega$  to zero within a few mK. The Ti/Au TES is biased by a voltage  $V_b$  and the current through the TES is measured with a low-impedance Superconducting Quantum Interference Device (SQUID) amplifier. The applied bias voltage  $V_b$  results in heating of the absorber/thermometer assembly to a temperature within the superconducting-to-normal transition region of the TES. At this operating point the heat flow via the heat link equals the Joule power dissipated in the TES. Radiation impinging on the absorber causes a small temperature rise. The resistance of the thermometer rises, causing the current and heat dissipation to drop. Through this electrothermal feedback (ETF) the sensor is self-stabilizing and the time constant to return to the setpoint is reduced with respect to the intrinsic  $C/G$  (heat capacity / thermal conductance) time constant. By integration of the current (difference) signal, the energy of the incoming radiation can be determined.

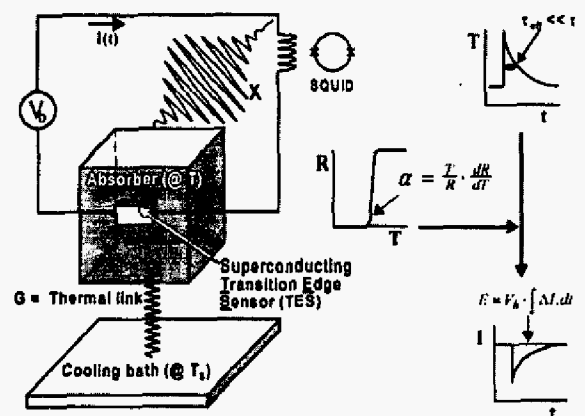


Fig. 1: Basic operating principle of a microcalorimeter with TES readout.

### Single pixel performance

In recent years the focus has been on the optimization and the understanding of single pixel microcalorimeters. The best sensors, as produced and measured at SRON, have an energy resolution  $\Delta E_{\text{FWHM}} = 3.9$  eV for 5.9 keV photons,

combined with an effective time constant of 150  $\mu$ s. Similar sensors equipped with a high (90%) absorption efficiency Bi absorber showed an energy resolution of 5.3 eV [4]. This level of performance is very close to the theoretical limit and is amongst the best-reported values in literature [3, 5, 6] and close to the XEUS requirements. The experience with these sensors forms the basis for the design of the array structures.

### Microcalorimeter arrays

In order to fulfill the performance specifications, such as energy resolution, time constant and efficiency, for each pixel, the design of the building element in a microcalorimeter array is faced with the following challenges:

- Each pixel should have the same thermal link to the cold bath, independent of the position in the array.
- The electrical and thermal cross talk between the pixels must be small enough not to degrade the energy resolution.
- Efficiency requirements lead to a close-packed design. Space must be available for electrical wiring and thermal connections.

The basic pixel design is illustrated in Fig 2. The Ti/Au TES and Cu/Bi absorber are supported by a low-stress silicon-rich  $\text{Si}_x\text{N}_y$  membrane, which in turn is connected to a silicon support structure by 4 beams; one at each corner of the membrane. These beams provide the required thermal link to the cold bath. The absorber has a mushroom shape to allow for close packing and still have enough space available for connecting wiring and membrane tuning.

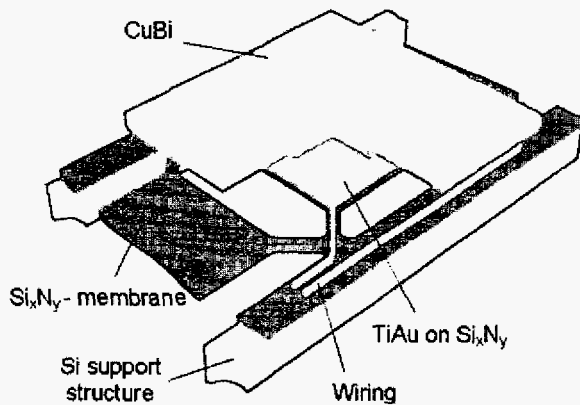


Fig. 2: Conceptual design of an array pixel. The overhanging Cu/Bi absorber allows for close packing. The slots in the  $\text{Si}_x\text{N}_y$  membrane to tune the heat conductance and the connecting wiring are located underneath the absorber. Note that the aspect ratio is distorted. The lateral pixel size is about 250  $\mu$ m and the absorber thickness about 7  $\mu$ m.

Two processing routes were investigated to realize 5x5 arrays that can later be extended to the 32x32 pixels required for XEUS [7]. The two routes differ in the way the

silicon support structure is realized. The fabrication of the metal structures (Ti/Au TES and Cu/Bi absorber) is identical. In order to optimize the design of pixels and large-format arrays, an elaborate finite element model has been constructed. This model uses low-temperature (0.01 – 1 K) material parameters of the materials used, mostly measured within the context of this research.

In the bulk micromachining route deep, vertical slots are etched in the backside of a Si (110) wafer by KOH etching. Fig. 3 shows a cross-sectional drawing of a resulting array. The advantage of bulk micromachining is the relative simplicity. Disadvantages are vulnerability to mechanical stress and finite thermal conductance of the silicon beams that tends to limit the array size. It was hoped that the very small surface roughness of the (111) beam walls would give a very long phonon mean free path and thereby good heat conduction. Measurements indicate that the phonon mfp is 110  $\mu$ m for a 40  $\mu$ m wide beam, which is not sufficient for a 32x32 array. To improve cooling of the beams, 70% of their area is now covered with a 0.6  $\mu$ m thick Cu coating, which gives excellent thermal properties.

The other processing route is based on surface micromachining. A shallow cavity underneath each pixel is created by utilizing a patterned poly-Si sacrificial layer. The cavity is formed at the end of the production process, either by wet TMAH etching from the front side or through dry etched access holes from the backside of the wafer. A schematic drawing is shown in Fig. 4. In comparison with the (uncoated) bulk micromachined structure the expected thermal conductance is higher, which reduces thermal cross talk. Furthermore, the structure is mechanically more rigid and it opens the way to bury electrical wiring under the pixel. With a given line width limitation this enables formation of a larger array.

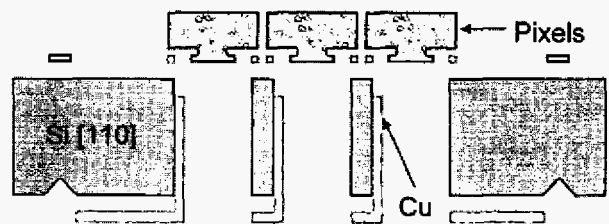


Fig. 3: Schematic side view of a bulk micromachined pixel array

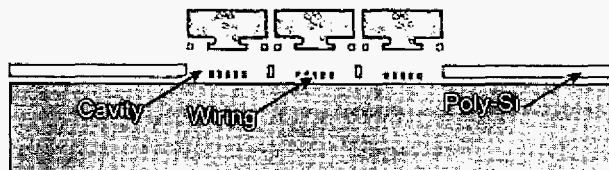


Fig. 4: Schematic side view of a surface micromachined pixel array

A potential problem arises from the sacrificial layer etching, which takes 5–8 hours in TMAH at 85 °C. Metal layers are prone to chemical attack by the TMAH and the characteristics of the Ti/Au bilayer are changed by interdiffusion occurring during the TMAH etch. The shift in the transition temperature can be taken into account however and we found that a coating of 5 nm Ti protects all metal layers in the pixels sufficiently. Problems with stiction of the membranes to the bottom of the shallow cavity were solved by either using tiny bumps under the membrane or by ending the release step with a freeze-drying process.

### 3. FABRICATION

Prototype 5x5 pixel microcalorimeter arrays were fabricated with three pixels (side, center, corner) connected and fully operational. The other membranes are equipped with heaters, enabling operation under a condition of dissipating bias power in the whole array. Fig. 5 shows photographs of both types of arrays.

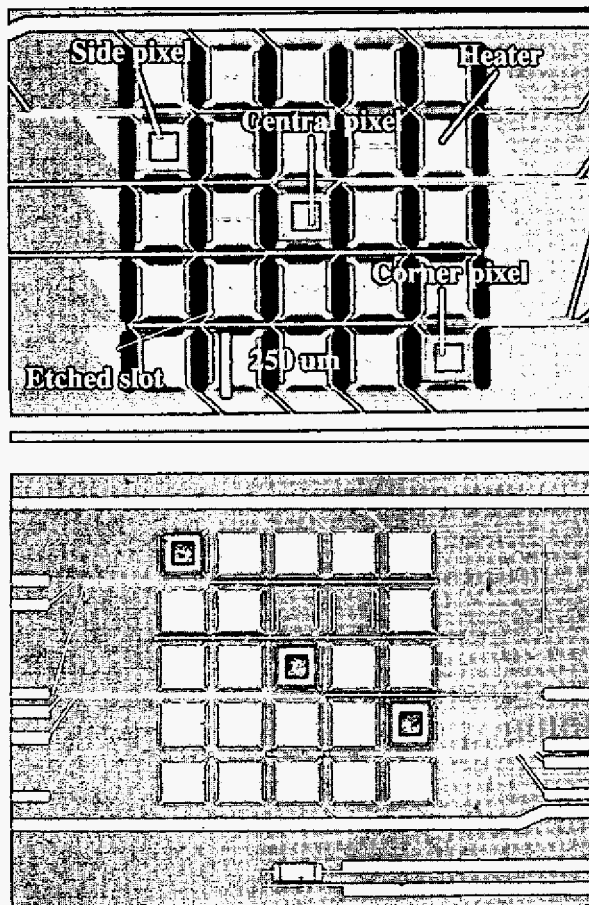


Fig. 5 Photographs of fabricated bulk (top) and surface (bottom) micromachined prototype arrays with three functional pixels.

As can be seen in the lower part of Fig. 5, two pixels in the surface micromachined array are not released. This is believed to be due to metal traces on the poly-Si sacrificial layer from an imperfect previous processing step, which protect the poly-Si from etching in TMAH.

### 4. RESULTS

The arrays were characterized by Resistance-Temperature (R-T) traces, Current-Voltage (I-V) traces and pulse response under voltage bias for 5.9 keV X-rays. R-T traces are shown in Fig. 6, I-V traces in Fig. 7. A reasonable uniformity of response was observed. The I-V traces reveal a good temperature coefficient of resistance of about 70 – 100 under bias conditions. The bias power in the transition equals about 2 – 4 pW/pixel, depending on the geometry of etched slots. This is considerably lower than expected when compared to measurement results obtained on single pixels on large closed membranes. An extensive study was done on the thermal conductance of  $\text{Si}_x\text{N}_y$  membranes, using results of microcalorimeter structures and special test structures, containing tiny heaters and thermometers. The thermal conductance of our  $\text{Si}_x\text{N}_y$  layers on Si [110] substrates and on poly-Si appeared to be 4 times lower than of previously used  $\text{Si}_x\text{N}_y$  on Si [100] wafers. Further research is going on to investigate whether the difference is due to the substrate or due to a difference in the deposition parameters. In parallel, the geometry of the pixels has been adapted in order to tune the bias power to about 10 pW, required for the desired time constant of 100  $\mu\text{s}$ . Fig. 8 shows a photograph of a fabricated bulk micromachined array dimensioned for 10 pW bias power. The silicon support beams are much wider. Furthermore, the slots along the sides of the silicon nitride membranes have been omitted, i.e. the membranes are connected directly to the silicon support. Tuning of the heat conductance is now done by changing the overlap of the TESs and the silicon beams. Measurements results on these new arrays are expected soon and will be available at the time of the conference.

X-ray energy resolution measurements were performed on several pixels of the bulk micro-machined arrays. The response time of the pixels varies from 0.2 to 3  $\mu\text{s}$  for membrane legs with a width ranging from 200 to 15  $\mu\text{m}$ , respectively. The best resolution measured for a few pixels equals 5 eV FWHM at 6 keV. This is very comparable to SRON's results of fully analyzed single pixel microcalorimeters, which show a resolution down to 3.9 eV at 5.9 keV. Clearly the X-ray resolution of array pixels is already close to what has been achieved for fully analyzed pixels. Still, improvement is needed with respect to reproducibility of the measurements. Work has started to improve the EM-shielding in the experimental set-up and move to fully differential cabling and electronics.

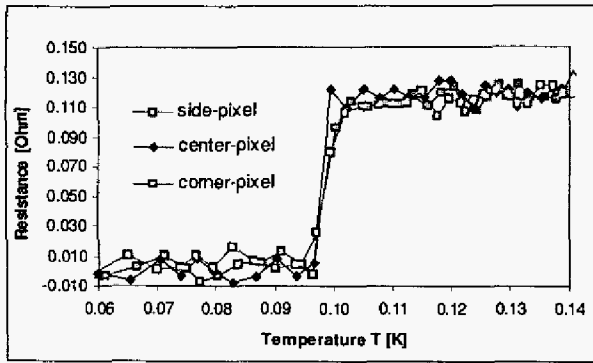


Fig. 6 Measured  $R(T)$  curves for each of the three pixels in the bulk micromachined array.

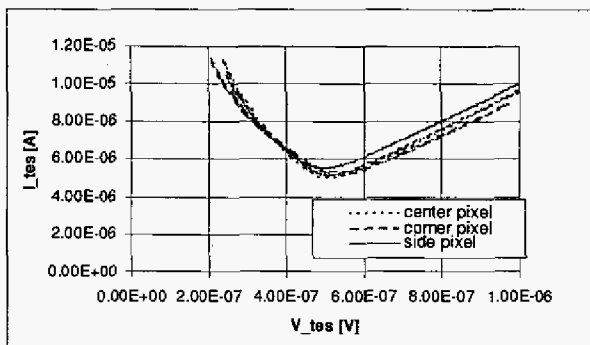


Fig. 7 Measured  $I-V$  curves for the pixels in the bulk micromachined array.

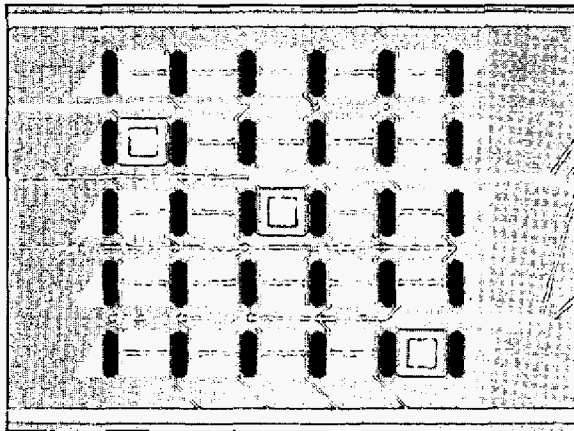


Fig. 8 Photograph of fabricated bulk micromachined prototype arrays with increased thermal conductance to the cold bath by omitting the slots in the silicon nitride membranes. As a result, the silicon support beams between the pixels can be somewhat thicker.

## 5. CONCLUSIONS

Two processing routes were investigated to realize  $5 \times 5$  X-ray spectroscopic detector arrays that can later be extended to  $32 \times 32$  pixels required for XEUS. Prototype arrays were

fabricated with three pixels (side, center, corner) connected and fully operational. The power needed to operate the TES at 100 mK is 2–4 pW/pixel whereas they were designed for 10 pW; giving a thermal response time 3 to 4 times slower than intended. After extensive analysis and experiments it was concluded that the thermal conductance of the  $\text{Si}_x\text{N}_y$  membranes lower than that of previously used membranes. So far it is not clear whether this difference originates from the crystal orientation of the substrate (Si [110] and poly-Si instead of Si [100]) or from changed deposition conditions. In parallel a new design was made where the slots in the  $\text{Si}_x\text{N}_y$  membranes are omitted. A positive side effect is that the silicon support beams can be somewhat wider. It is expected that the redesign will reduce the thermal response times from 300 to 400  $\mu\text{s}$  down to the required 100  $\mu\text{s}$ .

$R(T)$  and  $I-V$  curves were measured for each of the three pixels (side, center, corner) of the fabricated arrays, showing that the uniformity over the array is quite good. X-ray energy-resolution measurements were performed on several pixels. The best resolution measured for a few pixels equals 5 eV FWHM at 6 keV.

## ACKNOWLEDGEMENTS

Part of this work is supported by a research grant from the Dutch Organization for Scientific Research (NWO) and by contract 15850/01/NL/HB of ESA's technological research program.

## REFERENCES

- [1] S.H. Moseley, J.C. Mather, and D. McCammon, "Thermal detectors as X-ray spectrometers," *J. Appl. Phys.* **56**, 1257, 1984.
- [2] K.D. Irwin, "An application of electrothermal feedback for high resolution resolution cryogenic particle detection", *Appl. Phys. Lett.* **66**, 1998, 1995.
- [3] W. Bergman Tiest, M. Bruijn, H. Hoovers, P. de Korte, J. van der Kuur, and W. Mels, "Understanding TES microcalorimeter noise and energy resolution," *Proc. LTD-10, Nucl. Instr. and Meth. A* **520**, 329, 2004.
- [4] W.M. Bergmann Tiest, H.F.C. Hoovers, M.P. Bruijn, W.A. Mels, M.L. Ridder, P.A.J. de Korte, and M.E. Huber, *Proc. 9th Int. Workshop on Low Temperature Detectors*, Madison, 22-27 July 2001, AIP Conf. Proc. 605, p. 199, 2002.
- [5] K.D. Irwin, G.C. Hilton, J.M. Martinis, S. Deiker, N. Bergren, S.W. Nam, D.A. Rudman, and D.A. Wollman, *Nucl. Instr. Meth. A* **444**, p. 184, 2000.
- [6] C.K. Stahle, P. Brekosky, E. Figueroa-Feliciano, F.M. Finkbeiner, J.D. Gygax, M.J. Li, M.A. Lindeman, F. Scott Porter, and N. Tralshawala, *SPIE Proc.* **4140**, p. 367, 2000.
- [7] M.P. Bruijn, N.H.R. Baars, W.M. Bergmann Tiest, A. Germeau, H.F.C. Hoovers, P.A.J. de Korte, W.A. Mels, M.L. Ridder, E. Krouwer, J.J. van Baar, and R.J. Wiegerink, "Development of an array of transition edge sensors for application in X-ray astronomy", *Nucl. Instr. and Meth. A* **520**, 443, 2004.